JOURNAL OF MATHEMATICAL PSYCHOLOGY 33, 1–35 (1989)

Constant Volume Operators and Lateral Inhibition

JOHN I. YELLOTT, JR.

Cognitive Sciences Department,
University of California, Irvine

Constant volume (CV) operators are nonlinear image processing operators in which the area covered by the pointspread function around each point in the input image varies inversely with the light intensity at that point. This operation is designed to make spatial resolution increase with retinal illuminance, but it proves to have unexpected side-effects that mimic other important properties of human spatial vision, including Mach bands and Weber's law. Mach bands are usually attributed to lateral inhibition in the retina, and when retinal image processing is modeled by a linear operator they imply such inhibition, since they cannot be produced by a nonnegative impulse response. CV operators demonstrate that Mach bands and other high-pass filter effects can be created by purely positive pointspread functions, i.e., without inhibition. This paper shows in addition that if one attempts to combine lateral inhibition with a CV operation, the results are dramatically wrong: the edge response always contains Mach bands that bulge in the wrong direction. Thus within the nonlinear theoretical framework provided by CV operators, lateral inhibition is neither necessary nor sufficient for modeling Mach bands and other high-pass filter properties of spatial vision.

1. INTRODUCTION

1.1. *Overview*

Much of current visual theory is based on operators that transform an input image $I(x, y)$ into an output image $\mathbf{O}[I](x, y)$ by convolving I with some impulse response—in other words, shift-invariant linear operators. In particular, a standard device for modeling the retinal stage of early visual processing is a circular-symmetric linear operator of the form

$$\mathbf{O}[I](x, y) = \int_{-\infty}^{\infty} \int_{-\infty}^{\infty} I(x', y')\, S[(x-x')^2 + (y-y')^2]\, dx'\, dy', \qquad (1)$$

where the impulse response has a profile like a Mexican sombrero, e.g., $S =$ a difference-of-Gaussians (Enroth-Cugell and Robson, 1966), or $S =$ the negative Laplacian of a Gaussian (Marr and Hildreth, 1980). For such impulse responses

Reprint requests should be sent to the author at the Cognitive Sciences Department, University of California, Irvine, CA, 92717. I am endebted to Tom Cornsweet for creating the idea of constant volume operators, and to A. Ahumada, D. Bosman, S. Reuman, and the Odetics Corp. for interest and assistance. Research was supported by NASA Grants NCA2-5 and NCA2-Or345-301.

0022-2496/89 $3.00

the linear operation represented by (1) creates a low-frequency falloff in the modulation transfer function and, as a consequence, "edge enhancement" (i.e., the response to a luminance step is not monotonic, but contains a local minimum on the low side of the edge and a local maximum on the high side). Both effects resemble important properties of human spatial vision: the low-frequency falloff exhibited by psychophysical spatial contrast sensitivity functions (Shade, 1956; Van Nes and Bouman, 1967), and the Mach bands seen at edges (Mach, 1865; Ratliff, 1965).

These perceptual phenomena have generally been attributed to a process of lateral inhibition in the retina. That process is represented in the linear model (1) by the presence of negative lobes in the impulse response—the brim of the sombrero. Within the framework of linear systems theory these negative lobes are the only natural way to create Mach bands and other high-pass filter effects, because the edge response of a shift-invariant linear operator must be monotonic if its impulse response is entirely nonnegative.

To see explicitly why this is so, suppose the input image I in (1) is a vertical edge of the form $I(x', y') = L$ for $x' \leqslant 0$; $I(x', y') = L + D$ for $x > 0$. Then the output image is

$$\begin{aligned}
\mathbf{O}[I](x, y) &= \int_{-\infty}^{\infty} \int_{-\infty}^{0} L \cdot S[(x-x')^2 + (x-y')^2]\, dx'\, dy' \\
&\quad + \int_{-\infty}^{\infty} \int_{0}^{\infty} (L+D) \cdot S[(x-x')^2 + (y-y')^2]\, dx'\, dy' \\
&= L \int_{-\infty}^{\infty} \int_{-\infty}^{\infty} S[x'^2 + y'^2]\, dx'\, dy' \\
&\quad + D \int_{-\infty}^{\infty} \int_{0}^{\infty} S[(x-x')^2 + (y-y')^2]\, dx'\, dy' \\
&= LV + D \int_{-\infty}^{\infty} \int_{-x}^{\infty} S[x'^2 + y'^2]\, dx'\, dy',
\end{aligned}$$

where V is the total volume under the impulse response $S[x'^2 + y'^2]$. If the impulse response is nonnegative the integral in the last line is a nondecreasing function of x, so the profile of the edge response can only contain Mach bands if S is sometimes negative.

So when retinal image processing is modeled by linear operators, Mach bands and lateral inhibition seem inseparably linked in an if-and-only-if relationship. But that relationship is binding only for linear operators. This paper deals with a class of simple nonlinear operators—"constant volume" (CV) operators—that produce Mach bands without inhibition (i.e., with purely positive pointspread functions) and simultaneously model a surprising range of additional visual phenomena (Cornsweet and Yellott, 1985; Yellott, 1987). The fact that CV operators can create Mach bands and other high-pass filter effects without lateral inhibition has already

been established in the earlier papers just cited. The main original point of the present paper is to show that for this class of operators, lateral inhibition is not simply *unnecessary* for creating these effects, but also rather dramatically *insufficient*: we show that combining lateral inhibition with a CV operation leads to an edge response whose Mach bands bulge in the wrong direction (as illustrated in Fig. 8). In other words, if one begins by thinking about retinal image processing in terms of CV operators rather than linear operators, the same perceptual phenomena that force one to postulate lateral inhibition in the linear case acquire exactly the opposite significance: instead of implying lateral inhibition, they rule it out.

This incompatibility between lateral inhibition and the CV operation is demonstrated in Sections 3.6 (for deterministic input images) and 4.3 (for images with Poisson noise). The rest of the paper puts these results in context by reviewing properties of CV operators that were originally derived in the two earlier papers. First Section 1.2 outlines the class of visual phenomena that CV operators are intended to model. Then Section 2 defines CV operators, including the important Gaussian case, and compares them to linear operators. Section 3 describes the consequences of applying CV operators to deterministic images, and Section 4 describes their consequences for images containing Poisson noise—images that model the quantum catches of photoreceptors. That section also shows how CV operators are motivated by signal detectability considerations combined with the statistical properties of light.

It should be noted that the theory of CV operators is still in rudimentary form: as we shall see, many mathematical problems remain to be solved. One purpose of this paper is to call these problems to the attention of mathematical psychologists. Readers interested in them are referred to Yellott (1987) for a fuller discussion.

1.2. *Psychophysical Motivation*

From a psychophysical standpoint, CV operators are interesting because they show that a single fixed-parameter mechanism can duplicate most of the properties of spatial vision that are usually attributed to retinal processes, including the changes in those properties that are produced by changes in the prevailing illumination level. As that level rises from starlight to normal room light (i.e., by a factor on the order of 10^6), human spatial vision undergoes three major changes.

First, spatial resolution improves: the spatial contrast sensitivity function (CSF) shifts to the right along the spatial frequency axis (Van Nes and Bouman, 1967) so that the highest resolvable frequency (i.e., visual acuity) increases roughly as the square root of retinal illuminance. (Figure 3 in Thomas, 1975, illustrates this growth for grating acuity. Figures 11.2 and 11.3 in Pirenne, 1967, make the same point for acuity measured with Landolt rings.)

Second, the shape of the CSF changes from that of a low-pass filter to that of a bandpass filter. (Van Nes and Bouman, 1967, show that for mean retinal illuminances below .1 td the CSF decreases monotonically with frequency. For illuminances

above 1 td, sensitivity peaks around 3 cycles/deg and falls off monotonically for higher and lower frequencies.)

Third, the visibility of objects becomes independent of their absolute luminance and comes to depend only on their contrast against the background (e.g., Barlow, 1957; Glezer, 1965). That is, the detectability of a luminance change from I to $I + cI$ in some region of the visual field eventually depends only on the contrast c, once I is sufficiently high. ("Sufficiently" depends on the size of the region: smaller regions require a larger I value.) This third fact of vision is, of course, Weber's law, and one of its corollaries is that the visibility of objects is independent of their illumination and depends only on their reflectance—a valuable property for visual systems subject to the vicissitudes of the sun.

(None of these changes can be attributed simply to the transition from rod to cone vision. Pirenne (1967, Fig. 11.3) shows that acuity grows with retinal illuminance for both the rod and the cone systems separately. Hess and Nordby (1986) show that observers who possess only rod vision still have a CSF that changes from low pass to bandpass as mean illuminance rises, so that change cannot be due entirely to the rod–cone transition. Aguilar and Stiles (1954) show that increment thresholds in rod vision only start to obey Weber's law at background levels above .01 td; and Glezer (1965) shows for foveal (pure cone) vision that Weber's law emerges only above a background level that is higher the smaller the test spot.)

Linear operators offer no natural account of these illuminance-related changes in the properties of spatial vision. Linear models do predict some growth in spatial resolution with retinal illuminance simply because increased illuminance improves the signal-to-noise ratio of the photoreceptor quantum catch. But that improvement can only cause the spatial CSF to translate upwards (in the convential log–log plot); it cannot predict the horizontal shift along the spatial frequency axis that also occurs. To achieve such a shift in a linear model the width of the impulse response must decrease as retinal illuminance rises, and of course linear operators do not automatically adjust themselves in that fashion—some additional mechanism must be postulated to make them do so. The same is true of the change from low-pass to bandpass filter characteristics: for a linear operator this change implies that the shape of the impulse response is different at different light levels. In other words, a fixed-parameter linear operator can only model the CSF at a single mean illuminance level, and nonlinear mechanisms must be evoked to account for the way the CSF changes from one level to another.

In much the same way, Weber's law can only be incorporated into linear models by grafting on a nonlinearity, e.g., a compressive transformation at the level of the photoreceptors. But one such appendage is not enough: another must be added to explain why Weber's law only begins to hold above a certain luminance level, and another still to explain why the scope of Weber's law should depend on the size of the detection target.

So viewed from the standpoint of linear systems theory, spatial vision appears to undergo a complex set of unrelated changes as the illumination level rises from

starlight to daylight. Are these changes really as unrelated (and unmotivated) as they seem from a linear perspective? CV operators show that from another perspective, all of them can be viewed as consequences of a single operation whose "real purpose" is to maximize spatial resolution in the face of photon noise. Essentially, a CV operator is simply a mechanism that adjusts the area of the pointspread function to match the prevailing light level (in a signal detectability sense explained in Section 4)—a mechanism that causes spatial resolution to rise with retinal illuminance. Intuitively one might expect that the only consequence of this operation would be the increase in acuity that is built into it from the start. However, it turns out (rather surprisingly) that the same operation automatically gives rise to edge enhancement and other high-pass filter effects, and also to Weber's law—including that law's dependence on luminance and target size. And when applied to images with photon noise, it causes the CSF to change shape from low pass to bandpass as retinal illuminance rises from scotopic to mesopic levels. In other words, all of the basic properties of spatial vision reviewed earlier can be duplicated by a single fixed-parameter CV operator—a single image processing operation, motivated by the intrinsic noisiness of light.

The basic idea of CV operators is that each point in the input image creates a pointspread function whose area varies inversely with the input image intensity at that point. This mechanism was originally suggested by the psychophysical fact that the size of the spatial summation area (Ricco's area) in the human retina shrinks as the mean luminance level rises. (Barlow, 1958, shows this for the extrafovea retina. Glezer, 1965, shows it for the fovea.) Consequently we originally referred to this class of operators as "intensity dependent spatial summation" operators (in Cornsweet and Yellott, 1985). However, in this paper (and in Yellott, 1987) I adopt the name "constant volume" operator, following a suggestion by Bosman (Bosman *et al.*, 1985). This name seems appropriate because it captures the fundamental difference between our nonlinear operators and linear operators. As noted in Section 2.3, the latter can be thought of as "constant area" operators.

2. The Structure of Constant Volume Operators

2.1. *Definition*

In the same way that (1) defines a continuous linear operator **O**, a continuous constant volume operator **O** is defined as

$$\mathbf{O}[I](x, y) = \int_{-\infty}^{\infty} \int_{-\infty}^{\infty} I(x', y') \times S[I(x', y') \cdot \{(x-x')^2 + (y-y')^2\}]\, dx'\, dy', \tag{2}$$

where $I(x', y')$ is an input image (I is nonnegative, since it represents light intensity), $\mathbf{O}[I](x, y)$ is the corresponding output image (sometimes denoted

$\mathbf{O}[I(x', y')](x, y)$, when the arguments of I must be identified explicitly), and S is a real-valued function (of a single real variable) called the "spread function" of the operator $\mathbf{O}$. We assume that $S[x^2 + y^2]$ is integrable over the x, y plane. A given CV operator is entirely characterized by its spread function, just as a linear operator is characterized by its impulse response. Formally it is possible for S to take on both negative and positive values, but as we shall show, for image processing purposes S must be nonnegative to produce sensible results.

Figure 1 illustrates the structure of discrete CV operators—the kind that could actually grow in a retina or be constructed by an engineer. An input image (here, a sharp edge) is recorded by an array of photoreceptors, and each receptor gives rise to a pointspread function whose height at the center is directly proportional to its quantum catch, but whose volume is a constant independent of the catch. That is, if the quantum catch of the receptor centered at position (x', y') is I, the pointspread function created by that receptor (i.e., the value contributed to each output point (x, y)) is $I \cdot S[I\{(x-x')^2 + (y-y')^2\}]$. Integrating this pointspread function over the x, y plane yields a constant value V_s (the volume under $S[x^2 + y^2]$) that is independent of I. Consequently the "equivalent area" under the pointspread function generated by each photoreceptor (i.e., the volume V_s divided by the center height $I \cdot S[0]$) is inversely proportional to the input intensity I. The output image $\mathbf{O}[I](x, y)$ is simply the sum of the pointspread functions generated by all the photoreceptors. Equation (2) thus represents the continuous case of this operation, i.e., the limiting case where the receptors are negligibly small.

2.2. *Saturation*

The major difference between the discrete and continuous cases is that in the discrete case a CV operator can "saturate." Saturation occurs when the input intensity at a photoreceptor becomes so large that the pointspread function is narrower than

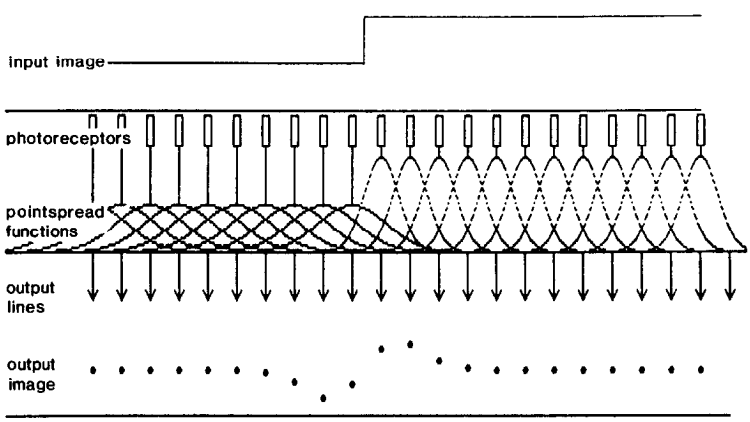

FIG. 1. Structure of a discrete constant volume operator with a Gaussian spread function.

the receptor itself. Once this level is reached the receptor outputs the same value for all higher input intensities. If the entire input image exceeds the saturation level, the output for all input images is a uniform field, so the CV operator creates total blindness beyond that point. This saturation effect has no analog in the case of continuous CV operators, where the receptor is treated as an infinitesimal point.

Saturation thus forces one to exercise some discretion about generalizing from continuous CV operators to their discrete analogs. But this is only a problem at high light levels. All the results reported here assume input images that are uniformly below the saturation level, so that the continuous model (2) gives physically meaningful results. The potential working range of any CV operator can be deduced from the basic fact that when the light level rises by a factor L, the area covered by the pointspread shrinks by the factor $1/L$. If the area of the pointspread function for a 1-photon quantum catch is $A(1)$ times the area of one receptor, then $A(L)$, the area for a catch of L quanta, covers $A(1)/L$ receptors. So saturation is complete when $L = A(1)$. The next section gives an example of the working range of a specific CV operator.

2.3. *The Gaussian Constant Volume Operator*

Figure 1 illustrates the Gaussian CV operator, i.e., the case where the spread funtion S is given by

$$S[x^2 + y^2] = (1/2\pi\sigma^2) \exp[(-1/2\sigma^2)(x^2 + y^2)].$$

For this CV operator the output image $O[I](x, y)$ is

$$\int_{-\infty}^{\infty} \int_{-\infty}^{\infty} I(x', y')(1/2\pi\sigma^2) \times \exp[(-1/2\sigma^2)\, I(x', y')\{(x-x')^2 + (y-y')^2\}]\, dx'\, dy'. \tag{3}$$

Here the constant pointspread volume $V_s = 1.0$. This case is uniquely convenient from an analytic standpoint because the Gaussian is the only separable function that is circularly symmetric, so that one can solve Eq. (2) explicitly for a large class of input images. In this paper we focus on the Gaussian case because it is the only CV operator whose properties have been worked out for both deterministic (Cornsweet and Yellott, 1985) and photon-noisy (Yellott, 1987) images. However, for the deterministic case one can show that the general properties of CV operators are largely independent of the exact choice of S, and this is almost certainly true for noisy images as well, although for the most part that remains to be proved.

The parameter σ in (3) determines the equivalent area covered by the pointspread for every input intensity I: that area is $2\pi\sigma^2/I$. Once this area is fixed for any I value (say, $I = 1$), it is fixed for all values, and the numerical properties of the Gaussian CV operator are completely determined.

To calculate the saturation level of the Gaussian CV operator we can use the fact that 99% of the volume of a circular-symmetric Gaussian probability density

function is enclosed by a circle of radius 3.03σ. If the distance unit is photoreceptor diameters, then the effective area covered by the Gaussian pointspread for a quantum catch of one photon (i.e., $A(1)$ from the last section) is $\pi(3.03\sigma)^2$, so the operator will be completely saturated once the quantum catch/receptor reaches that value. Yellott (1987) shows that σ must be around 100 receptor diameters to match human psychophysical data. For that σ the saturation level is 288, 426, or as a conservative order of magnitude value, 10^5 quanta/receptor.

2.4. *Constant Volume and Constant Area Operators*

Before describing the properties of CV operators, let us compare their basic structure with that of linear operators (see Fig. 2). A linear operator such as (1) describes an operation in which each photoreceptor (say, the receptor at location (x', y')) gives rise to a pointspread function of the form $I \cdot S[(x-x')^2+(y-y')^2]$, where I is the input intensity at (x', y'). If the volume under S (i.e., the integral of $S[x^2+y^2]$ over the x, y plane) is V_s, then the volume under the pointspread function for input intensity I is $I \cdot V_s$, and the center height of the pointspread is $I \cdot S[0]$. So for linear operators it is the area under the pointspread function (i.e., volume/center height) that remains constant across all values of the input intensity. Thus the names "constant volume" for operators of the form (2) and "constant area" for operators of the form (1) capture the only essential structural difference between image processing by CV operators and image processing by shift-invariant linear operators. Figure 2 illustrates this point by showing on the left the pointspreads generated for a low- and a high-intensity input value by a CV operator (here, the Gaussian case), and on the right, the pointspreads generated for the same low and high values by a linear operator (here, the linear operator whose impulse response is a difference-of-Gaussians).

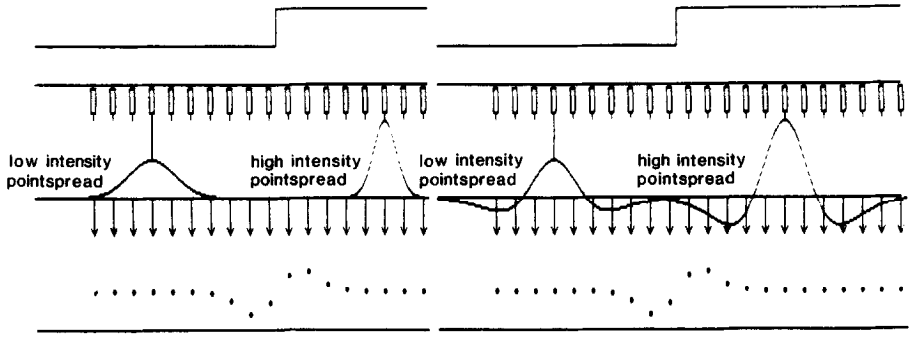

FIG. 2. Comparison between constant volume operators (left side, Gaussian spread function) and shift-invariant linear operators (right side, difference-of-Gaussians impulse response). CV operators cause the pointspread area to vary inversely with the input intensity at each point. A linear operator causes the pointspread area to remain constant across all input intensities.

3. Properties of CV Operators for Deterministic Input Images

3.1. *Overview*

This section describes the consequences of applying CV operators to deterministic images. We have shown in earlier papers (Cornsweet and Yellott, 1985; Yellott, 1987) that CV operators create edge enhancement (Mach bands) and other high-pass filter effects without lateral inhibition, i.e., with pointspread functions that are never negative. The main point of the present paper is to show that for CV operators, lateral inhibition is not simply unnecessary for modeling visual high-pass filter effects, but also inadaquate, in the sense that a CV operator based on a spread function with negative lobes (e.g., a difference-of-Gaussians) creates output images that are qualitatively incompatible with the facts of vision. That point is demonstrated for deterministic images in Section 3.6. Sections 3.2–3.5 set the stage for this demonstration by reviewing the basic properties of CV operators applied to deterministic input images. Unless otherwise noted, these preliminary results are all derived in the two earlier papers, so we include here only a few illustrative proofs. The material in Section 3.6 is new, and there we give a complete treatment.

3.2. *Response Compression*

For any CV operator, all uniform field input images (i.e., $I(x', y') \equiv I > 0$) give rise to the same uniform output image. (This is easily shown by setting $I(x', y')$ in (2) equal to any constant I and making the change of variables $u = (x' - x)\sqrt{I}$, $v = (y' - y)\sqrt{I}$.) For the Gaussian case the constant output level is 1.0. In general it is the volume under the spread function $S[x^2 + y^2]$.

So for all CV operators every uniform field input image, whatever its intensity, yields the same output value. For the Gaussian operator it can also be shown (Yellott, 1987) that all possible input images are compressed into the same narrow range of output values: the output range is 0 to $2.1 + 0.7(\ln[\sigma])$. (For $\sigma = 100$, the upper limit is 5.3.) From a design standpoint this is an important feature. A major problem for all visual systems, both biological and artificial, is that the luminance of natural scenes varies over the course of a day by at least 8 log units. This enormous dynamic range cannot be transmitted directly from an eye to a brain, or from a TV camera to a computer—it must be somehow compressed. Linear operators offer no solution to this problem: at best they can only compress the output to purely uniform fields by making it identically zero. CV operators automatically cause the outputs for all potential input images to fall in the same narrow range of values. Moreover this is not accomplished by simply rescaling the output (i.e., by simply changing the gain). Instead, as input luminance rises, the output image values remain in the same numerical range, but these numbers carry an increasing amount of information about high spatial frequencies in the input image.

(An important open problem is to show that all CV operators create response compression, regardless of the form of the spread function. It should be noted that the proof of this for the Gaussian case assumes physically possible input images,

whose values must be nonnegative integers since they represent numbers of absorbed photons. This excludes input images of the form $I(x, y) = 1/(x^2 + y^2)$, which could cause infinite output values.)

3.3. *Sinusoidal Grating Response: Bandpass Filtering*

For input images consisting of low-contrast sinusoidal gratings (i.e., $I(x', y') = L(1 + m \cdot \cos 2\pi f x')$, with $m \leqslant 0.1$) the output of the Gaussian CV operator is approximately sinusoidal (with an error on the order of m^2) and takes the form $1 + g(f/\sqrt{L}) \cdot m \cdot \cos 2\pi f x$, where the function g is given by Eq. (4). Thus for gratings with contrasts in the neighborhood of psychophysical detection thresholds, one can define a modulation transfer function (MTF, output contrast/input contrast as a function of the input spatial frequency f). The fact that the modulation transfer function here takes the form $g(f/\sqrt{L})$ implies that visual acuity (defined by any high-frequency cutoff of the MTF) varies as the square root of the mean illuminance level L.

Figure 3 shows the MTF of the Gaussian CV operator for five mean illuminance levels, plotted in the conventional way on log–log coordinates. In this plot the MTF shifts bodily to the right as L increases: the peak frequency is proportional to $\sqrt{L}$. Remarkably, the MTF for the Gaussian CV operator at any fixed mean luminance has the same form as that of a linear operator whose impulse response is the negative LaPlacian of a Gaussian: Marr and Hildreth's (1980) famous "Del^2-G" operator. That is, the MTF for the Gaussian CV operator is

$$g(f/\sqrt{L}) = 2\pi^2\sigma^2(f/\sqrt{L})^2 \exp[-2\pi^2\sigma^2(f/\sqrt{L})^2]. \tag{4}$$

Thus it creates a low-frequency falloff in the MTF (i.e., acts like a bandpass linear filter) despite the fact that its pointspread functions are never negative. In

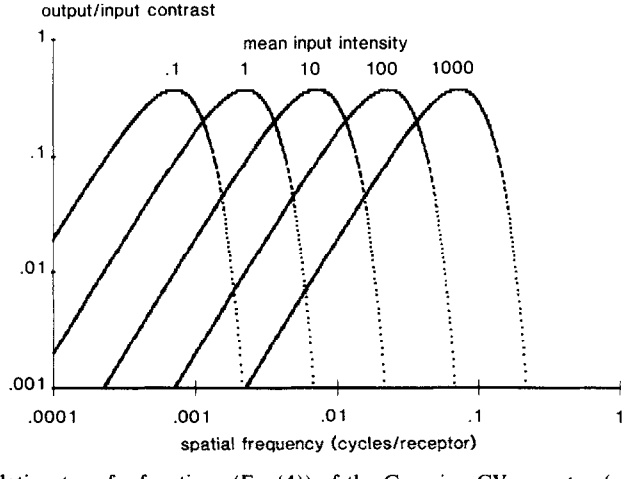

FIG. 3. Modulation transfer functions (Eq. (4)) of the Gaussian CV operator ($\sigma = 100$) at different mean input intensity levels (for deterministic input images).

other words, it mimics the effects of lateral inhibition even though it involves no inhibition—only positive spatial summation.

The MTFs in Fig. 3 differ from psychophysical CSFs in two important respects: they fail to exhibit a change from low-pass to bandpass filter characteristics as mean illuminance rises, and the peak value of the MTF is the same at all illuminances, whereas the peak sensitivity in the human CSF grows from about 10 (threshold contrast = 10%) to more than 100 (threshold contrast < 1%) as mean illuminance rises from absolute threshold to 100 td. As we see in Section 4, both of these effects prove to be natural consequences of CV operators once photon noise is taken into account.

3.4. *Edge Responses: Mach Bands and Weber's Law*

The fact that the MTFs in Fig. 3 exhibit low-frequency attenuation suggests that CV operators should create Mach bands, and this proves to be true in quite a remarkable way. Figure 4 shows the output of a Gaussian CV operator when the input image is a sharp edge, i.e., a step from illuminance L to $L + D$. Three response profiles are shown, for steps from 1 to 1.5, 10 to 15, and 100 to 150 quanta/input point. Thus the contrast at the edge is same for all three input images, but the mean illuminance increases by a factor of 10 from one to the next. Two facts are evident: the edge response contains Mach bands in all cases, and the maximum and minimum values of the output are the same for all three input images. All that changes with the mean illuminance are the widths of the Mach bands, and the locations of their peak and trough: those extreme values move closer to the edge itself as L increases. In other words, the amplitude of the edge response obeys Weber's law. This is a general property of CV operators, regardless of their spread function.

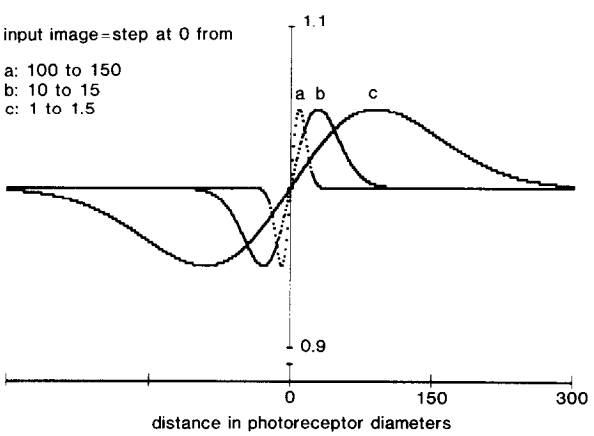

FIG. 4. Edge response profiles for the Gaussian CV operator ($\sigma = 100$) at different input intensity levels (Eq. (5) with $L = 1$, 10, and 100, and $D/L = 0.5$). The Mach bands have a constant peak amplitude because D/L is constant: this is the Weber's law property of CV operators.

To explore this point a bit, consider first the Gaussian CV operator. Suppose the input image is a vertical edge separating two uniform fields, i.e., $I(x', y') = I(x') = L$ for $x' \leqslant 0$; $I(x') = L + D$ for $x' > 0$. (CV operators are invariant under translations and rotations, so it is sufficient to consider only this special case.) For this input image the output image (i.e., the solution to (3)) is quickly found to be

$$\mathbf{O}[I](x, y) = N(x/\sigma)\sqrt{L+D}] + N[-(x/\sigma)\sqrt{L}], \tag{5}$$

where N is the cumulative normal distribution function:

$$N[z] = \int_{-\infty}^{z} (1/\sqrt{2\pi}) \exp[(-1/2)x^2]\, dx.$$

(Since the output image $\mathbf{O}[I](x, y)$ varies only with x, we write it as $\mathbf{O}[I](x)$ in what follows.) Then differentiation shows that the maximum of (5) occurs at $x = x_{\max} = \sigma\sqrt{(1/D)\ln(1 + D/L)}$, and the value of that maximum is

$$\mathbf{O}[I](x_{\max}) = N[\sqrt{(1 + L/D)\ln(1 + D/L)}] + N[-\sqrt{(L/D)\ln(1 + D/L)}]$$

which is a function only of the Weber fraction D/L. The same sort of argument shows that this is also true of the minimum value of the edge response. Thus if the output of this CV operator is fed into an edge detecting mechanism that registers an edge whenever its input exceeds the baseline input value by some criterion amount, that mechanism would behave according to Weber's law.

Of course in psychophysical experiments, Weber's law only starts to hold when the background luminance exceeds some critical level—a level that is inversely related to the size of the detection target. We will see in a moment that this is exactly the behavior predicted by CV operators, once we take into account the fact that actual detection targets have a finite size, rather than consisting of infinitely extended edges. First, however, we will show how the Weber law just obtained for the Gaussian CV operator can be generalized to all CV operators.

For this purpose we need a technical result which plays a fundamental role in the analysis of CV operators—a result we call the "Scaling Theorem." It describes the effect of multiplying the input image by a constant, as would happen if the illumination falling on a scene changed while the reflectances of objects in the scene remained the same.

THEOREM 1. *For any positive constant c and any input image $I(x', y')$ the output of any CV operator satisfies the relationship*

$$\mathbf{O}[c \cdot I(x', y')](x, y) = \mathbf{O}[I(x'/\sqrt{c}, y'/\sqrt{c})](x\sqrt{c}, y\sqrt{c}). \tag{6}$$

(In other words, multiplying all the input intensity values by a factor c has the same effect as expanding the input image by the factor $\sqrt{c}$ along both axes (or contracting it, when $c < 1$), applying $\mathbf{O}$ to that image, and then undoing the expansion by shrink-

ing the output image by the factor $1/\sqrt{c}$. *Hence the name Scaling Theorem: changing the illumination level changes the spatial scale of the operator—high spatial frequencies at high light levels are treated like low spatial frequencies at low levels.*)

Proof. From the definition (2) the right side of (6) is

$$\int_{-\infty}^{\infty}\int_{-\infty}^{\infty} I(x'/\sqrt{c},\, y'/\sqrt{c})\cdot S[I(x'/\sqrt{c},\, y'/\sqrt{c}) \times \{(x'-x\sqrt{c})^2+(y'-y\sqrt{c})^2\}]\, dx'\, dy'.$$

Making the change of variables $u = x'/\sqrt{c}$, $v = y'/\sqrt{c}$, we have

$$\int_{-\infty}^{\infty}\int_{-\infty}^{\infty} cI(u, v)\cdot S[cI(u, v)\{(x-u)^2+(y-v)^2\}]\, du\, dv$$

which is the left side of (6). ∎

This simple theorem is the key to a general treatment of CV operators. As an illustration, we use it to show the following:

THEOREM 2. *Suppose* $I(x', y')$ *is an input image consisting of a straight edge separating a uniform field of intensity* L *from a field of intensity* $L+wL$. *Then for any CV operator the maximum and minimum values of the output to* $I(x', y')$ *are independent of* L *and depend only on the Weber fraction* w.

Proof. Because CV operators are invariant under translations and rotations, it is sufficient to consider only vertical edges of the form $I(x', y') = I(x') = L$ for $x' \leqslant 0$; $I(x') = L + wL$ for $x' > 0$. Suppose $V(x')$ is a vertical edge image defined by $V(x') = 1$ for $x' \leqslant 0$; $V(x') = 1 + w$ for $x' > 0$. Assume that the maximum value of the output $\mathbf{O}[V(x')](x)$ occurs at $x = x_{\max}$ and that the minimum value occurs at $x = x_{\min}$. Let $I(x') = L$ for $x' \leqslant 0$ and $L + wL$ for $x' > 0$. Then $I(x') = L \cdot V(x')$, and so from Theorem 1 we have

$$\mathbf{O}[I(x')](x) = \mathbf{O}[L\cdot V(x')](x) = \mathbf{O}[V(x')/\sqrt{L})](x\sqrt{L}) = \mathbf{O}[V(x')](x\sqrt{L}).$$

(The last equality holds because here $V(x'/\sqrt{L}) = V(x')$.) The maximum value of the last expression in this string of equalities occurs at $x\sqrt{L} = x_{\max}$, and its minimum at $x\sqrt{L} = x_{\min}$, and so the maximum (minimum) output to $I(x')$ occurs at $x = x_{\max}/\sqrt{L}$ ($x = x_{\min}/\sqrt{L}$) and has the same value there that the output to $V(x')$ has at $x_{\max}$ ($x_{\min}$). ∎

Note that we have also shown that for all CV operators, the distance between the locations of the peak and trough of the Mach band and the edge itself both decrease as $1/\sqrt{L}$—in effect, the width of the Mach bands varies as $1/\sqrt{L}$.

3.5. *Increment Threshold and t.v.i. Curves*

We have just seen that the maximum and minimum values of a CV operator's response to an edge obey Weber's law, but the propositions of these extreme values change with the background illuminance level, moving closer to the edge as that level increases. Now consider a typical increment threshold experiment in which a target of some fixed size (e.g., a square) and illuminance $L + D$ is surrounded by a background of illuminance L. We measure the value of D required for the target to be just detectable and repeat this measurement for different values of L to obtain a "threshold vs intensity" (t.v.i.) curve, usually plotted as log (threshold D) vs log(L). Weber's law holds when this t.v.i. curve becomes a straight line with slope 1.0.

Figure 5 shows what the Gaussian CV operator implies for such an experiment. Each graph shows the output response profile for a square target of fixed width and

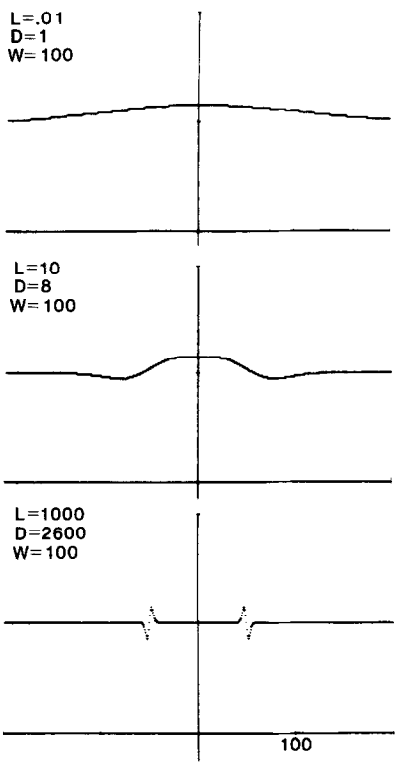

FIG. 5. Response profiles for the Gaussian CV operator applied to a square spot of intensity $L + D$ surrounded by a background of intensity L. Spot width is held constant at 100, and D is adjusted to produce a constant peak response value of 1.15. At low background levels (top graph) the response is simply a broad shallow bump. At moderate levels (middle graph) it resembles a classical sombrero-shaped receptive field. At sufficiently high levels (bottom graph) the response has the same value inside the spot as outside; only the Mach bands at the edges signal the presence of the spot. Once this level is reached the spot's visibility is governed by Weber's law.

intensity $L+D$ surrounded by a background of intensity L. (Equation (4.6) in Yellott, 1987, gives an analytic expression for the response to such targets.) The three graphs correspond to three different values of the background: $L=0.1$ in the top panel, $L=10$ in the middle panel, and $L=100$ in the lowest panel. The D value in all three cases was adjusted to make the maximum value of the output equal to a constant, as though we were finding the increment threshold for each background intensity. (The threshold value was arbitrarily chosen to be 1.15, but that was only a matter of convenience—the form of the results would be the same for any threshold value.) One can see that at the lowest background level the response to the target is simply a broad bump, with no evident edge enhancement: the Mach bands are so broad and shallow as to be invisible. As the background level rises the Mach bands become narrower, and the response to the target spot begins to look like the profile of a classic center-surround receptive field. Finally, at the highest background level, the Mach bands have become sufficiently narrow that they do not overlap at all. Now the response in the center of the target is at the uniform field value, and the maximum response occurs at the peaks of the Mach bands, where as we have seen it is governed by Weber's law. So for this background level, and all higher ones, the increment threshold for this target will obey Weber's law.

Figure 6 shows the t.v.i. curve for this target (width $W=100$ receptor diameters), and two others, one smaller ($W=10$), the other larger ($W=1000$). ("Threshold" was arbitrarily defined by a peak response value of 1.15.) All three curves contain an early region where increment threshold does not change with background intensity (as though threshold were limited by "dark light," although in fact there is none here), and then beyond some background level each curve bends upwards and eventually asymptotes in a straight line with slope 1.0—Weber's law. The only effect of target area is that the smaller the target, the higher the background level must be before Weber's law starts to hold. So the CV operator duplicates the general form of t.v.i. curves obtained in psychophysical increment threshold experiments.

Of course from a psychophysical standpoint these results are only suggestive,

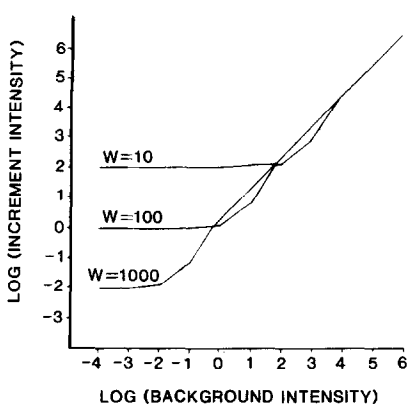

FIG. 6. Threshold vs background intensity curves for deterministic test spots of different sizes. (W, spot width in receptor diameters. See text for details.)

because we have not yet included photon noise in our analysis—there is nothing in the model so far to limit detection, so we cannot make meaningful comparisons between CV predictions and experimental results. However, as we see in Section 4, when photon noise is taken into account, the t.v.i. curves predicted by the Gaussian CV operator have the same general form as those in Fig. 6: for any test spot the t.v.i. curve obeys Weber's law above some level of background illuminance, and larger spots reach the Weber range sooner than smaller ones.

3.6. *CV Operators and Lateral Inhibition*

So far we have concentrated on CV operators with nonnegative spread functions, i.e., operators that model a retinal process of purely positive spatial summation, with no lateral inhibition. We have seen that such operators duplicate the high-pass filter effects, such as Mach bands, that are usually attributed to lateral inhibition, and at the same time automatically model two major visual phenomena associated with changes in the prevailing light level: improvement in spatial resolution with increasing mean luminance, and the emergence of Weber's law. Computer simulation indicates that these effects are all robust under changes in the exact form of the basic spread function S, so that it does not matter greatly whether S is Gaussian or exponential or any other plausible form, so long as it is nonnegative. A natural question at this point is whether it even matters that S be nonnegative. Examination of the proof of Theorem 1 (the scaling Theorem) shows that it does not depend on that assumption, and since Theorem 2 follows from Theorem 1, it is also true that the edge response of a CV operator will continue to obey Weber's law even is S is sometimes negative. Cornsweet and Yellott (1985) derive the general form of the CV modulation transfer function from the Scaling Theorem as well, and show that it is always a function of the ratio $f/\sqrt{L}$, causing its high-frequency cutoff to increase as $\sqrt{L}$. So a CV operator with a sometimes-negative spread function will also imply that grating acuity should improve as the square root of mean retinal illuminance. So one might suspect that a sensible model for early visual processing could be constructed by combining the familiar concept of lateral inhibition with the CV notion of a pointspread function whose area varies inversely with the input intensity.

Somewhat surprisingly, this is not the case. In fact exactly the opposite is true: for CV operators, the assumption of lateral inhibition leads to consequences that are blatantly at odds with the facts of visual perception and that would be quite disastrous in an artificial image processing system. We demonstrate this first for the special case in which the spread function is a difference-of-Gaussians and then show that the defects of that operator are common to all CV operators in which the spread function consists of a positive central region surrounded by a negative zone.

Consider first a CV operator in which the spread function S is a difference-of-Gaussians, as illustrated in Fig. 7. Specifically, we suppose that

$$S[x^2+y^2] = (1/2\pi)(1/\alpha)^2 \exp[(-1/2)(1/\alpha)^2 (x^2+y^2)] - (1/2\pi)(1/\beta)^2 \exp[(-1/2)(1/\beta)^2 (x^2+y^2)];$$

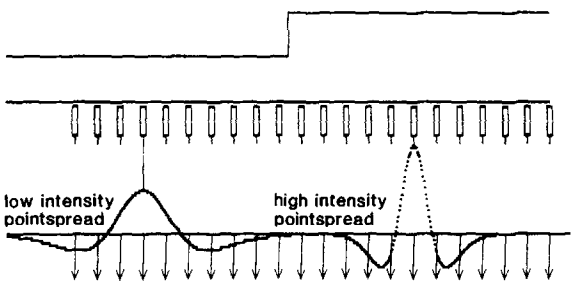

FIG. 7. A CV operator with lateral inhibition: the spread function S is a difference-of-Gaussians.

i.e., S is the difference between two bivariate normal densities with standard deviations α and β. This function has been widely used to model lateral inhibition in the retina (e.g., for modeling the receptive fields of X-type ganglion cells in Enroth-Cugell and Robson, 1966, and many subsequent papers.) For that purpose we require $\beta > \alpha$. (Marr and Hildreth, 1980, show that when $\beta = 1.6\alpha$, a difference-of-Gaussians is practically indistinguishable from their Del^2-G function.) We consider the CV operator generated by this spread function, which we will call $\mathbf{D}_{\alpha,\beta}$:

$$\begin{aligned}\mathbf{D}_{\alpha,\beta}[I(x', y')](x, y) = \int_{-\infty}^{\infty}\int_{-\infty}^{\infty} I(x', y')\,(1/2\pi) \\ \cdot\Big[(1/\alpha^2)\exp[(-1/2\alpha^2)\cdot I(x', y') \\ \cdot\{(x-x')^2+(y-y')^2\}] - (1/\beta^2)\cdot\exp[-(1/2\beta^2)\cdot I(x', y') \\ \cdot\{(x-x')^2+(y-y')^2\}]\Big]\,dx'\,dy'. \qquad (7)\end{aligned}$$

Now if we denote the Gaussian CV operator (3) with scale parameter σ by $\mathbf{G}_\sigma$, it is evident from inspection that $\mathbf{D}_{\alpha,\beta}$ can be expressed in terms of $\mathbf{G}_\sigma$:

$$\mathbf{D}_{\alpha,\beta}[I](x, y) = \mathbf{G}_\alpha[I](x, y) - \mathbf{G}_\beta[I](x, y). \qquad (8)$$

Consequently from results already obtained for the Gaussian CV operator $\mathbf{G}_\sigma$ we can immediately write down the response of the difference-of-Gaussians CV operator $\mathbf{D}_{\alpha,\beta}$ for the same input images. In particular, using (5) we obtain the following edge response (i.e., the output to $I(x', y') = L$ for $x' \leqslant 0$, $I(x', y') = L + D$ for $x' > 0$):

$$\begin{aligned}\mathbf{D}_{\alpha,\beta}[I](x) = N[(x/\alpha)\sqrt{L+D}] + N[-(x/\alpha)\sqrt{L}] \\ - N[(x/\beta)\sqrt{L+D}] - N[-(x/\beta)\sqrt{L}]. \qquad (9)\end{aligned}$$

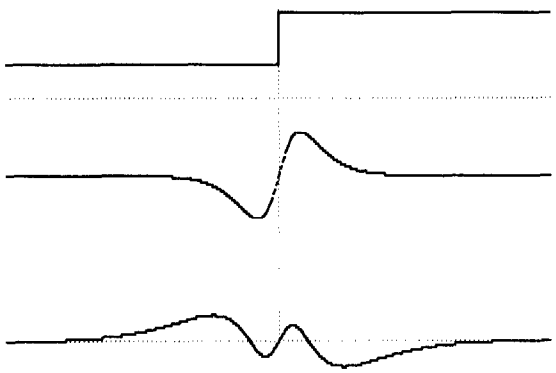

FIG. 8. Bottom graph, edge response profile of a lateral inhibitory CV operator (difference-of-Gaussians pointspread). The top graph illustrates the input image profile. The middle graph shows the response of a non-inhibitory (Gaussian pointspread) CV operator to the same edge.

The lower part of Fig. 8 shows this edge response for the case $\alpha = 1$, $\beta = 2$. The input edge here is a step from $L = 10$ to $L + D = 100$, illustrated at the top, and the curve in the middle is the Gaussian CV edge response (the response of $\mathbf{G}_1$). One sees immediately that the difference-of-Gaussians edge response is grotesque: it contains an extra pair of Mach bands bulging in the wrong direction! Analysis of Eq. (9) shows that these "wrong-way" Mach bands always appear for any α, β pair with $\alpha > \beta$.

Figure 9 illustrates a second (closely related) pathological consequence of combining lateral inhibition with a CV operation. It shows the modulation transfer function of $\mathbf{D}_{\alpha,\beta}$ (again, the case $\alpha = 1$, $\beta = 2$) for three values of the mean illuminance L. We see that these MTFs all contain a range of negative values,

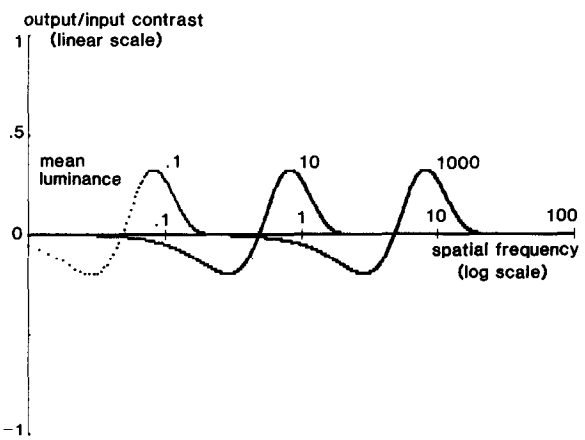

FIG. 9. Modulation transfer functions of the difference-of-Gaussians CV operator (Eq. (10)) at three different input intensity levels. Note the contrast reversal at low spatial frequencies.

meaning that for spatial frequencies in that range (which for this operator runs from 0 to $0.15\sqrt{L}$) the output to a sinusoidal grating input image is a sinusoid of the same frequency, but with reverse contrast—peaks in the input turn into troughs in the output, and vice versa. To show analytically how this comes about we apply (8) to a low-contrast sinusoidal grating, i.e., to an input image of the form $I(x', y') = L \cdot (1 + m \cdot \cos 2\pi f x')$, with $m \leqslant 0.1$. From the fact that the Gaussian CV operator response to this image is $1 + g(f\sigma/\sqrt{L}) \cdot m \cdot \cos 2\pi f x$, where g is given by Eq. (4), it follows that the response of the difference-of-Gaussians CV operator to the same image is $[g(f\alpha/\sqrt{L}) - g(f\beta/\sqrt{L})] \cdot m \cdot \cos 2\pi f x$. So the MTF of $\mathbf{D}_{\alpha,\beta}$ is

$$(2\pi^2 f^2/L) \cdot [\alpha^2 \cdot \exp(-2\pi^2\alpha^2 f^2/L) - \beta^2 \cdot \exp(-2\pi^2\beta^2 f^2/L)] \tag{10}$$

which is negative for $f < \sqrt{[(L/\pi^2(\beta^2 - \alpha^2)] \ln(\beta/\alpha)}$. So all difference-of-Gaussian CV operators (i.e., all scale parameter pairs α, β with $\beta > \alpha$) cause a contrast reversal for low spatial frequencies, (And since Marr and Hildreth's Del^2-G function is effectively equivalent to a difference-of-Gaussians with $\beta = 1.6\alpha$, the same will be true of it as well.)

Of course the difference-of-Gaussians family does not exhaust the set of all possible spread functions that might be used to model lateral inhibition. However, the following result shows that any spread function consisting of a positive (excitatory) central region surrounded by a negative (inhibitory) region will create wrong-way Mach bands in its edge response.

THEOREM 3. *Suppose a spread function* $S[x^2 + y^2]$ *is positive for* $\sqrt{x^2 + y^2} \leqslant C$ $(C > 0)$, *and negative for* $\sqrt{x^2 + y^2} > C$, *and the input image I is an edge of the form* $I(x', y') = L$ *for* $x' \leqslant 0$; $I(x', y') = L + D$ *for* $x' > 0$, *with* $D > 0$. *Let V denote the volume under the spread function S, and* $R(x)$ *the profile of the output image created when the CV operator with spread function S is applied to I (i.e.,* $R(x) = \mathbf{O}[I](x, 0)$*). Then* $R(0) = V$; $\lim_{x \to \infty} R(s) = V$; *and* $R(x) \leq V$ *for* $x > C/\sqrt{L}$. *Similarly,* $\lim_{x \to -\infty} R(x) = V$, *and* $R(x) > V$ *for* $x < -C/\sqrt{L}$.

(In other words, the profile of the edge response along the x axis is V at the edge itself and asymptotically V again at $\pm\infty$, dips below V on the high side of the edge for $C/\sqrt{L} < x < \infty$, and rises above V on the low side of the edge for $x < -c/\sqrt{L}$. Thus the edge response of any lateral inhibitory CV operator always contains the kind of wrong-way Mach bands illustrated in the bottom panel of Fig. 8.)

Proof. The edge response profile $R(x)$ is

$$R(x) = \int_{-\infty}^{\infty} \int_{-\infty}^{0} L \cdot S[L\{(x' - x)^2 + y'^2\}]\, dx'\, dy'$$

$$+ \int_{-\infty}^{\infty} \int_{0}^{\infty} (L + D) \cdot S[(L + D)\{(x' - x)^2 + y^2\}]\, dx'\, dy'. \tag{11}$$

Now in the first integral make the change of variables $u=(x'-x)\sqrt{L}$, $v=y'\sqrt{L}$, and in the second the same change using $\sqrt{L+D}$ instead of $\sqrt{L}$. Then we have

$$R(x)=\int_{-\infty}^{\infty}\int_{-\infty}^{-x\sqrt{L}} S[u^2+v^2]\,du\,dv$$

$$+\int_{-\infty}^{\infty}\int_{-x\sqrt{L+D}}^{\infty} S[u^2+v^2]\,du\,dv.$$

The first integral here is

$$V-\int_{-\infty}^{\infty}\int_{-x\sqrt{L}}^{\infty} S[u^2+v^2]\,du\,dv$$

and consequently we can write the edge response in form

$$R(x)=V+\int_{-\infty}^{\infty}\int_{-x}^{-x\sqrt{L}} \sqrt{L+D}\,S[u^2+v^2]\,du\,dv.$$

So the profile $R(x)$ is V at $x=0$, and its limit as $x\to+\infty$ (or $-\infty$) is also V. For $0<x<\infty$, $R(x)$ equals V plus the integral of $S[u^2+v^2]$ over the vertical strip defined by $-x\sqrt{L+D}\leqslant u\leqslant -x\sqrt{L}$, $-\infty<v<\infty$. If $-x\sqrt{L}\leqslant -C$ this strip falls entirely within the region where S is negative, so the integral is negative and $R(x)<V$. Thus for $x\geqslant C/\sqrt{L}$, $R(x)<R(0)=R(\infty)$, Q.E.D. The same argument applied for $x<0$ shows that there will be a symmetrical wrong-way Mach band on the low side of the edge. ▮

So for deterministic input images, all CV operators based on lateral inhibitory spread functions create an edge response containing Mach bands bulging the wrong way. Section 4.3 shows that this is also true of the expected response to a Poisson noisy edge.

4. CV Operators and Photon-Noisy Images

4.1. *Overview*

Now we consider input images in which the deterministic values $I(x', y')$ are replaced by random variables $Q(x', y')$ corresponding to the quantum catches at each photoreceptor during some fixed period of time. The $Q(x', y')$ are assumed to be mutually independent, and each has a Poisson distribution with expected value $q(x', y')=E\{Q(x', y')\}$. The mean value function q will be referred to as the "expected input image." The output image $\mathbf{O}[Q](x, y)$ is now a spatial stochastic process, and interest centers on its mean and variance at each point. The mean value function $E\{\mathbf{O}[Q](x, y)\}$ will be called the "expected output image."

Our main concern here is to show that for Poisson noisy input images, CV operators with nonnegative spread functions create results consistent with the properties of human spatial vision, whereas spread functions with negative lobes lead to distinctly nonvisual results. The first point has already been demonstrated in an earlier paper (Yellott, 1987). That paper derives expressions for the mean and variance of the Gaussian CV operator's response to uniform fields and for its expected response to sinusoidal gratings and circumscribed test spots. These results allow one to determine the input image parameters (grating contrast, etc.) needed to discriminate test images from uniform fields, and consequently to compare those parameter values to the results of psychophysical experiments. The main results of that analysis are illustrated here in Figs. 10, 11, and 12. Altogether, they show that a Gaussian CV operator applied to noisy images duplicates the major qualitative properties of human spatial vision (as outlined earlier in Section 1.2) for retinal illuminance levels ranging from absolute threshold (ca. 10^{-4} td) to 10^{3} td. In that range it causes the CSF to rise and shift rightwards along the spatial frequency axis (Fig. 10), so that acuity rises overall by a factor on the order of 100, and peak contrast sensitivity grows from 10 to more than 100. It also causes the CSF to change shape from low pass to bandpass as the mean quantum catch rises above 1 quantum/receptor, so that Mach bands begin to appear at edges for retinal illuminances above 0.1 td (Fig. 11). And it causes spot detectability (the increment threshold) to obey the deVries–Rose law at low background levels and Weber's law at high levels, with the emergence of Weber's law coming sooner the larger the test spot (Fig. 12).

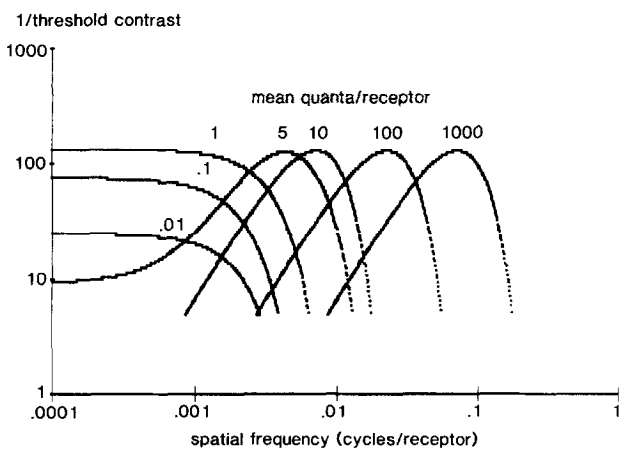

FIG. 10. Spatial contrast sensitivity functions of the Gaussian CV operator applied to photon-noisy sinusoidal gratings at different mean illuminance levels. A given curve shows the input contrast (sensitivity = 1/contrast) needed to produce a fixed level of detectability (peak $d' = \sqrt{2}$) in the output image as a function of input frequency.

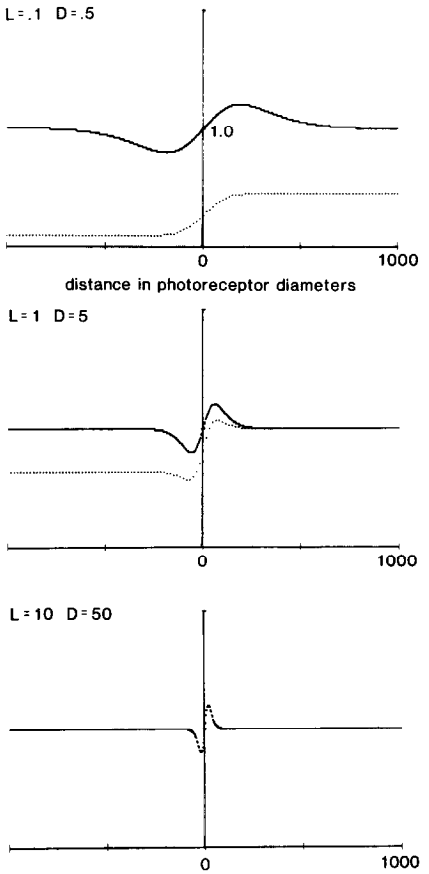

FIG. 11. Expected response profiles for the Gaussian CV operator ($\sigma = 100$) applied to photon-noisy edges (dotted curves) compared with its response to deterministic edges (solid curves). The input image is a step at zero from mean illuminance L quanta/receptor to $L + D$. When L is 10 or more the expected response for noisy input images coincides with the deterministic response (bottom graph). As L falls below 10 the expected response to noisy edges falls below the deterministic response (middle graph), and eventually its Mach bands disappear (top graph).

The derivation of these properties of the Gaussian CV operator in Yellott (1987) relies extensively on two general results established there:

(1) At moderate to high light levels (when $q(x', y')$ is uniformly $\geqslant 10$ quanta) the expected output image $E\{\mathbf{G}_\sigma[Q](x, y)\}$ is effectively the same as $\mathbf{G}_\sigma[q](x, y)$, i.e., the output image obtained by applying $\mathbf{G}_\sigma$ to the corresponding expected input image. (Figure 11 illustrates this point.) In other words, despite its nonlinearity the CV operator commutes with the expectation operator, as long as the light level is not too low. So for these input images, all of the results derived for the Gaussian

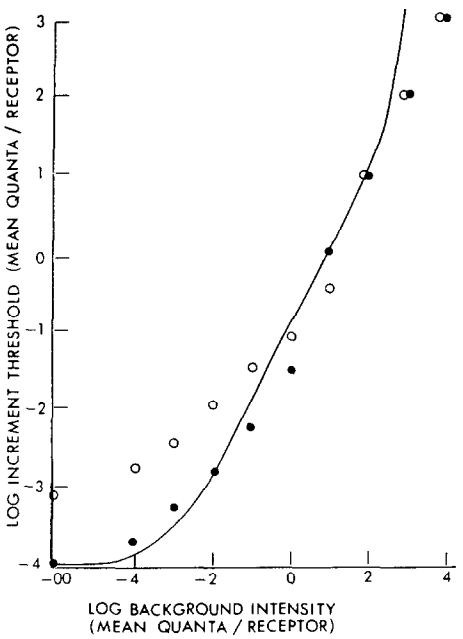

FIG. 12. Increment threshold vs background intensity (t.v.i.) predictions of the Gaussian CV operator G_{100} applied to photon-noisy images. Solid circles show the predictions for a 9° (diameter) test spot. The solid line is Aguilar and Stiles' (1954) t.v.i. curve for a 9° test spot detected by rods. The G_{100} predictions are generated by calculating the increment needed to achieve a d' of 6 at the response peak. (This d' was chosen to make G_{100}'s t.v.i. curve coincide with Aguilar and Stiles' at $L = 100$. The predicted threshold at $L = 0$ assumes a dark light of $10^{-4.4}$ mean quanta/photoreceptor. The dark light has no effect on the other predicted values.) Empty circles show G_{100}'s t.v.i. predictions for a smaller (0.8°) test spot. Note that the smaller spot requires a higher background intensity to reach its Weber's law range ($L = 100$ vs $L = 10$ for the 9° spot).

CV operator in the deterministic case can be carried over intact to the Poisson noisy case.

(2). At very low light levels ($q(x, y)$ uniformly $\leqslant 0.1$ quantum) the Gaussian CV operator becomes equivalent to the shift-invariant linear operator whose impulse response is the Gaussian spread function $S(r^2) = [1/(2\pi\sigma^2)] \exp(-r^2/2\sigma^2)$. Thus at low light levels $\mathbf{G}_\sigma$ acts like a linear filter.

Section 4.3 shows that these two properties are also true of the difference-of-Gaussians CV operator $\mathbf{D}_{\alpha,\beta}$. Consequently at moderate to high light levels that operator's expected output image for an edge input will contain wrong-way Mach bands, just as it does in the deterministic case, and the CSF will become negative (contrast reversal will occur) for low spatial frequencies. And at low light levels $\mathbf{D}_{\alpha,\beta}$ becomes equivalent to a linear operator with a difference-of-Gaussians impulse response, so its predicted CSF will exhibit low-frequency attenuation (bandpass filtering) in the illuminance range where the human CSF resembles that of a low-

pass filter. Thus for photon-noisy input input images at both high and low light levels, combining a difference-of-Gaussians spread function with the CV operation leads to output images that are qualitatively inconsistent with the facts of spatial vision. And Section 4.3 shows that these defects are common to all CV operators with spread functions that embody lateral inhibition.

Before turning to these points we first show how photon noise itself provides a rationale for CV operators.

4.2. *Photon Noise and CV Operators*

As Rose (1942, 1948) and deVries (1943) pointed out many years ago, the random nature of photon absorption imposes an ultimate limit on contrast detection in any visual system. If the illuminance (mean quantum catch per photoreceptor per unit time) in some portion of an image is I, the actual quantum catch in an area containing R receptors over any time interval T is a Poisson random variable with mean and variance equal to IRT. If one patch of retina containing R receptors receives illuminance I, and another patch of the same size receives illuminance $I+cI$ ($c>0$), the "brighter" patch can only be identified in any given time period if its actual quantum catch is larger. Using the normal approximation to the Poisson distribution it is quickly shown that for this minimal condition to be satisfied with a failure rate on the order of 1%, one needs a mean total quantum catch per time period on the order of

$$IR > 10/c^2. \tag{12}$$

Thus reliable detection of 100% contrast requires a mean total catch on the order of 10 quanta, 10% contrast requires 1000, etc. Current estimates indicate that the mean quantum catch of a single primate photoreceptor is about 4 photons per second per troland of retinal illuminance. (Baylor, Nunn, and Schnapf, 1984). Visually, a full second is rather a long interval: the temporal integration period of photoreceptors is more like a quarter-second at the very most. So as a rule of thumb we can say that individual receptors catch an average of one quantum per "visual time unit" for each troland of retinal illuminance. The working range of the human visual system spans about 10 log units, from 10^{-4} to 10^{6} td. Over that range the contrast threshold (for large targets) never exceeds 100% and generally is much lower (ca. 20% above 10^{-2} td, and 10% or less at higher levels) (e.g., Aguilar and Stiles, 1954.) When these parameters are combined with Eq. (12), it is obvious that over most of its operating range the visual system must be detecting contrast on the basis of the summed quantum catch of many photoreceptors: it must pool at least 10^5 receptors to detect 100% contrast at 10^{-4} td, at least 25,000 to detect 20% at 10^{-2} td, etc. It is only when the mean illuminance reaches 1000 td that 1% contrast can be detected on the basis of the quantum catch of a single receptor.

Spatial summation can thus be seen as a mechanism that is forced on the visual system by the statistics of light itself: it raises the effective quantum catch to an acceptable level by increasing the effective collection area. At the same time,

however, spatial summation limits spatial resolution, since two points cannot be resolved if both fall inside a common summation area. So while contrast sensitivity considerations dictate a large summation area, spatial resolution considerations dictate a small one. The signal detection requirement expressed by (12) suggests how this conflict should be resolved: to maximize spatial resolution across different light levels while maintaining a constant reliability of detection for any given contrast level, the quantum collection area R should vary inversely with the light level I. This is what CV operators are designed to accomplish automatically—in effect by causing each photoreceptor to vote on the proper size of the collection area, based on its own quantum catch.

The striking point, of course, is that a mechanism designed simply to match the spatial summation area to the prevailing light level (that is, to the prevailing signal-to-noise ratio of the photoreceptor quantum catch) should prove to automatically create edge enhancement and Weber's law—effects that are usually thought of as quite unrelated to photon noise.

Figures 13 and 14 illustrate how effective CV operators are at taming photon noise. The left hand panels in both figures show scan lines across simulated photon-noisy input images of a 50% contrast vertical edge at different light levels. The input image in each case was a 256×256 pixel image in which the value at each pixel was a Poisson random variable with a mean of L for pixels to the left of center (i.e., the left half of each image), and $L + D$ for pixels to the right of center. The ratio D/L was held constant at 0.5, and L ranged from 0.1 (in the top left panel of Fig. 13) to 10,000 (in the bottom left panel of Fig. 14). The figures show the actual pixel values along two horizontal lines across the input images. One can see that for L values below 10 (Fig. 13) the edge itself is essentially invisible in the input image, and even at $L = 100$ the jump in mean quantum catch to the right of the edge is still obscured by noise. The right hand panels show scan lines across the same images after they have been processed by the Gaussian CV operator (with $\sigma = 100$ pixels). For $L = 0.1$ and 1, where the operator is effectively linear, the output image has a monotonically increasing profile, so the only effect of the operator is to smooth out the noise. One can see that it does this quite effectively. (Yellott, 1987, shows that the variance of $\mathbf{G}_\sigma[Q](x, y)$ for any Poisson-noisy input image never exceeds $4.54/\sigma^2$. For $\sigma = 100$ this means that the standard deviation is at most 0.02, at any point in the output image, versus an average value on the order of 1.0. Computer simulations such as the one illustrated in Figs. 13 and 14 indicate that for most input images the actual output noise level is about 10 times smaller than this upper bound—the standard deviation is on the order of 0.002 rather than 0.02. For uniform field inputs it can be shown that the exact expression for the variance of $\mathbf{G}_\sigma[Q](x, y)$ is $(1/8\pi\sigma^2)[1 - \exp(-2L)]$, where L is the expected number of quanta at each input point. This means the output standard deviation for uniform fields is at most 0.002. It seems likely that this is also true for edge input images, but no analytic expression is known for the output variance in that case—or indeed, for any input image except uniform fields. (This is another important open problem.)

Once the input image quantum catch levels reach 10 or more mean quanta per

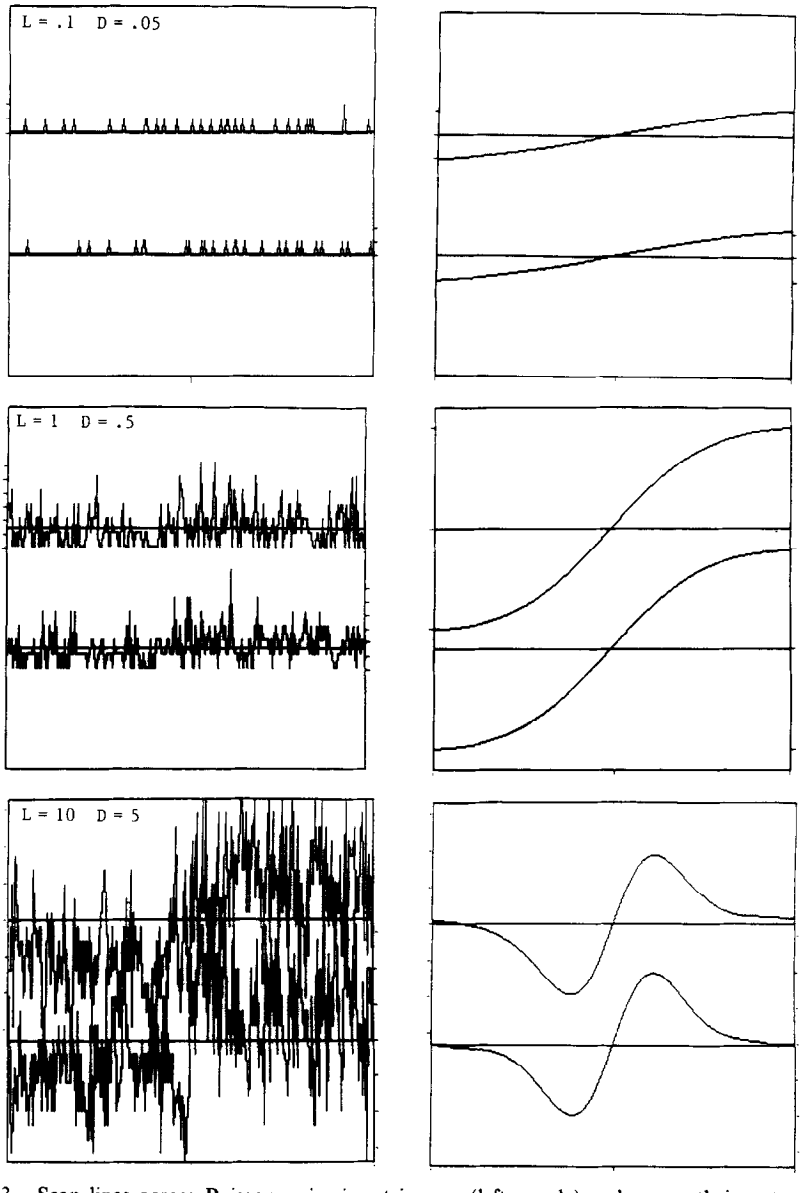

FIG. 13. Scan lines across Poisson noisy input images (left panels) and across their output images after application of the Gaussian CV operator $\mathbf{G}_{100}$ (right panels). The input images were noisy vertical edges with a mean value of L to the left of center and $L + D$ to the right of center, with $D/L = 0.5$ in all cases. Image size = 256 × 256 pixels. The left panels show the actual pixel values along two representative horizontal lines across the input image. Solid horizontal lines in the left panels indicate the mean input intensity level (i.e., $L + D/2$). In the top two panels the ordinate scale is the actual quantum catch: the scale for the upper scan line is shown on the left, and for the lower scan line on the right. In the bottom left panel the ordinate scale unit is 20% of the mean value; i.e., tick marks indicate $L + D/2$ plus or minus 20%, 40%, etc. The right hand panels show the output image values across the same two horizontal scan lines as those on the left. Solid horizontal lines here indicate the expected value of the edge response at the edge itself. In the bottom panel the tick marks indicate increments of 0.025 above and below 1.0.

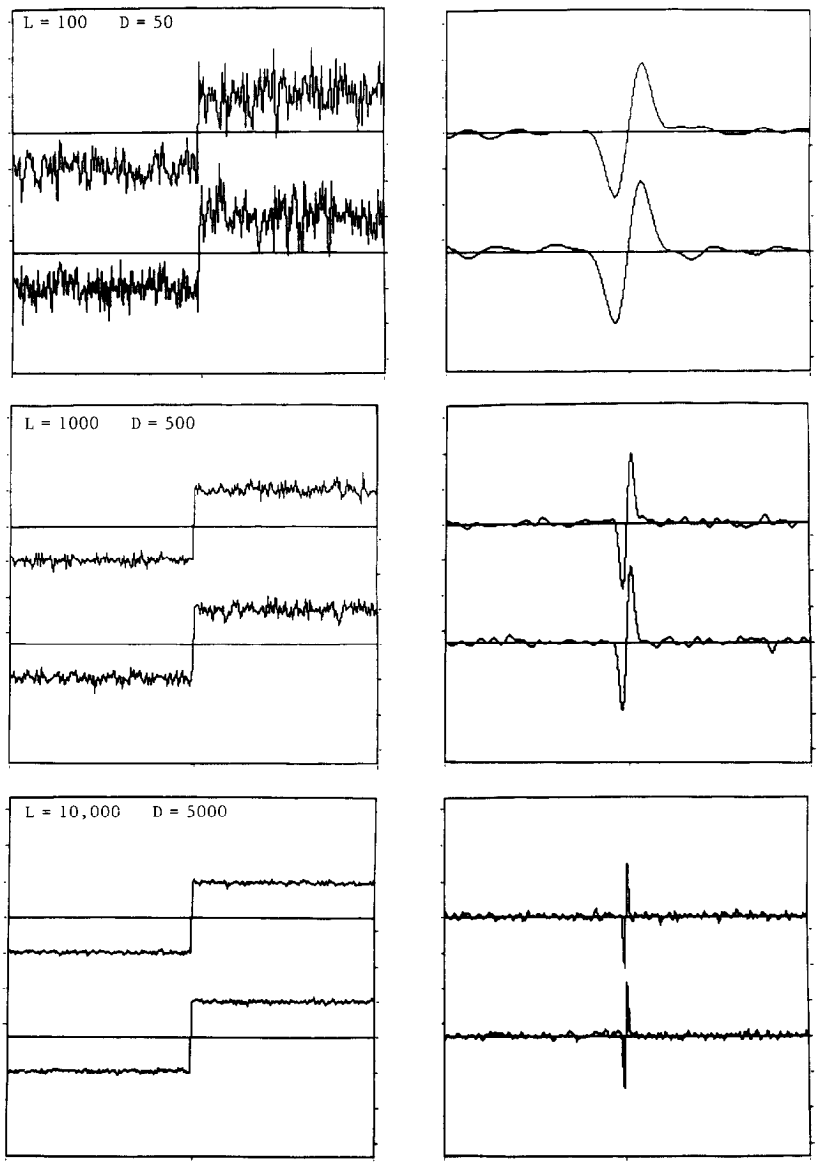

FIG. 14. Continuation of Fig. 13 at higher light levels.

pixel (Fig. 13, bottom panel, and all panels of Fig. 14) the CV operator's nonlinear properties are fully expressed—Mach bands begin to appear at edges, and their maximum and minimum values obey Weber's law. In this range the expected edge response is given by Eq. (5). The maximum and minimum values of that response do not depend on the σ parameter of the operator, but only on the contrast D/L.

Since the output image variance is bounded by $4.54/\sigma^2$, the output signal-to-noise ratio at the peak of the edge response can be made as large as desired by adjusting σ. In other words the Gaussian CV operator allows us to preset the detectability of fixed contrast edges (i.e., a fixed D/L ratio) at any desired level, and that level will remain constant across all illumination levels (i.e., for all values of L). Thus the visibility of any given reflectance ratio between an object and its background can be held constant despite changes in the prevailing illumination.

4.3. *Lateral Inhibitory CV Operators and Photon-Noisy Images*

Our goal now is to show that when the input image contains Poisson noise, any CV operator based on a lateral inhibitory spread function will create output images that are inconsistent with the facts of perception. The demonstration here follows the same pattern as that given in Section 3.6 for deterministic images: first we show that the difference-of-Gaussian CV operator $\mathbf{D}_{\alpha,\beta}$ will not work, and then we show that its defects are common to all CV operators whose spread functions have a positive central region surrounded by a negative zone. As before, we focus on the edge response.

As noted in Section 4.1, the Gaussian CV operator $\mathbf{G}_\sigma$ behaves quite differently for photon-noisy images at high and low light levels. At high levels its expected output images are essentially the same as those created in the deterministic case. More precisely, one can show (rather laboriously) the following:

THEOREM 4. *If the expected input image $q(x', y')$ is $\geqslant 10$ quanta for all (x', y'), then*

$$E\{\mathbf{G}_\sigma[Q](x, y) \approx \mathbf{G}_\sigma[q](x, y) \tag{13}$$

with an error of at most .045.

(Recall that the uniform field response of $\mathbf{G}_\sigma$ is 1.0, so the error in (13) is on the order of 5% at most. Computational experience shows that it decreases very quickly as q increases above 10.)

Proof. Yellott (1987, Theorem 1). ∎

Now suppose the input image Q is an edge: $q(x', y') = L$ for $x' \leqslant 0$; $q(x', y') = L + D$ for $x' > 0$, with $D > 0$. If $L \geqslant 10$, Theorem 4 combined with Eq. (8) allows us to write

$$\begin{aligned} E\{\mathbf{D}_{\alpha,\beta}[Q](x, y)\} &= E\{\mathbf{G}_\alpha[Q](x, y) - \mathbf{G}_\beta[Q](x, y)\} \\ &\approx \mathbf{G}_\alpha[q](x, y) - \mathbf{G}_\beta[q](x, y) \\ &= \mathbf{D}_{\alpha,\beta}[q](x, y), \end{aligned} \tag{14}$$

where $\mathbf{D}_{\alpha,\beta}[q](x, y)$ is the deterministic edge response given explicitly by Eq. (9) and illustrated in Fig. 8. So for high light levels the expected edge response of $\mathbf{D}_{\alpha,\beta}$ will contain the wrong-way Mach bands shown in that figure.

At very low light levels Mach bands are not present perceptually (Ratliff, 1965). Figure 11 shows that this fact is consistent with the Gaussian CV model: its Mach bands disappear when the expected quantum catch falls below 0.1 quantum/receptor. Yellott (1987) shows that when L and $L+D$ are both small enough that their squares can be treated as zero, the expected edge response of $\mathbf{G}_\sigma$ becomes

$$E\{\mathbf{G}_\sigma[Q](x, y)\} = L + D \cdot N(x/\sigma). \tag{15}$$

Consequently under the same conditions we have

$$E\{\mathbf{D}_{\alpha,\beta}[Q](x, y)\} = D \cdot [N(x/\alpha) - N(x/\beta)]. \tag{16}$$

Equation (16) is the edge response of a linear operator whose impulse response is a difference-of-Gaussians. It contains Mach bands whose maximum and minimum fall at

$$x = \pm\sqrt{2[\alpha^2\beta^2/(\beta^2 - \alpha^2)]\ln(\beta/\alpha)}.$$

So at low light levels the CV operator $\mathbf{D}_{\alpha,\beta}$ creates Mach bands, although none are present perceptually.

It remains now to show that the defects of the expected edge response of the difference-of-Gaussians CV operator are shared by any CV operator whose spread function embodies lateral inhibition. For the low-light defect this point is immediately obvious. Suppose that both L and $L+D$ are $\leqslant 0.1$. Then the probability of a quantum catch greater than 1 at any point is less than 0.005, so almost all photoreceptors catch either 1 quantum or none. If the receptor at (x', y') catches no quanta, it creates no pointspread function, and if it catches one it gives rise to the pointspread function $S[(x-x')^2 + (y-y')^2]$. Other pointspreads occur with negligible probability. So the effect of the CV operator at these light levels is essentially the same as that of the linear operator whose impulse response is $S[x^2 + y^2]$. (All this can be shown rigorously, but the point seems so intuitively clear that we spare the reader an elaborate calculation.) Consequently if the spread function S contains negative lobes that would create Mach bands in the edge response of a linear operator, it will also create such Mach bands in the edge response of a CV operator once the light level becomes sufficiently low. And that, of course, is precisely what one does not want a model to predict.

Now consider high light levels. For the difference-of-Gaussians CV operator the proof that wrong-way Mach bands will appear in the edge response at these levels was easy because of Theorem 4, i.e., because of the fact that for the Gaussian operator $\mathbf{G}_\sigma$ (and consequently $\mathbf{D}_{\alpha,\beta}$ as well) $E\{\mathbf{O}[Q](x, y) \approx \mathbf{O}[E\{Q\}](x, y)$. If this property could be shown to hold for all CV operators, regardless of the

spread function, then we could simply apply the deterministic-case Theorem 3 to the expected edge response for Poisson-noisy images and thereby show that all spread functions containing a positive central zone and a negative surround must create wrong-way Mach bands at high light levels. Unfortunately we have no proof that Theorem 4 holds for arbitrary spread functions. (This is perhaps the single most important open problem in the theory of CV operators.) Consequently we must take a longer route to obtain the following analog to Theorem 3:

THEOREM 5. *Suppose the spread function* $S[x^2+y^2]$ *is positive for* $\sqrt{x^2+y^2} \leqslant C$ *and negative for* $\sqrt{x^2+y^2} > C$; *and that the expected input image is the edge* $q(x, y) = L$ *for* $x \leqslant 0$, $q(x, y) = L+D$ *for* $x > 0$, *with* $D > 0$. *And suppose* L *is large enough that the cumulative Poisson distribution function* $P(Q \leqslant m) = \sum_{k=0}^{m} L^k(1/k!)\exp(-L)$ *can be replaced by the distribution function of a normal random variable with mean and variance* L. *Let* $R(x)$ *denote the profile of the expected output image along a line perpendicular to the edge, and* V *the volume under the spread function* $S[x^2+y^2]$. *Then* $R(0) = V = \lim_{x \to \pm\infty} R(x)$; $R(x) < V$ *for* $x > C$; *and* $R(x) > V$ *for* $x < -C$.

(In other words, when the expected quantum catch/receptor is on the order of 30 or more, the expected edge response of a lateral inhibitory CV operator will always contain wrong-way Mach bands.)

Proof. For this input image the expected output image is

$$\begin{aligned} E\{\mathbf{O}[Q](x, y)\} &= E\Bigg[\int_{-\infty}^{\infty}\int_{-\infty}^{\infty} Q(x', y') \\ &\quad \times S[Q(x', y')\{(x-x')^2+(y-y')^2\}]\,dx'\,dy'\Bigg] \\ &= \int_{-\infty}^{\infty}\int_{-\infty}^{0} \sum_{k=1}^{\infty} kS[k\{(x-x')^2+(y-y')^2\}] \\ &\quad \times L^k(1/k!)\exp(-L)\,dx'\,dy' \\ &\quad + \int_{-\infty}^{\infty}\int_{0}^{\infty} \sum_{k=1}^{\infty} kS[k\{(x-x')^2+(y-y')^2\}] \\ &\quad \times (L+D)^k\,(1/k!)\exp(-L-D)\,dx'\,dy'. \end{aligned}$$

Let $I1$ denote the first integral in the last equation, and $I2$ the second. Making the change of variables $u = (x'-x)\sqrt{k}$, $v = (y'-y)\sqrt{k}$, we have

$$I1 = \sum_{k=1}^{\infty} L^k(1/k!)\exp(-L)\int_{-\infty}^{\infty}\int_{-\infty}^{-x\sqrt{k}} S[u^2+v^2]\,du\,dv \tag{17}$$

and

$$I2 = \sum_{k=1}^{\infty} (L+D)^k (1/k!) \exp(-L-D) \int_{-\infty}^{\infty} \int_{-x\sqrt{k}}^{\infty} S[u^2+v^2]\, du\, dv$$

$$= \sum_{k=1}^{\infty} (L+D)^k (1/k!) \exp(-L-D) \left[V - \int_{-\infty}^{\infty} \int_{-\infty}^{-x\sqrt{k}} S[u^2+v^2]\, du\, dv \right]$$

$$= V[1-\exp(-L-D)]$$

$$- \sum_{k=1}^{\infty} (L+D)^k (1/k!) \int_{-\infty}^{\infty} \int_{-\infty}^{-x\sqrt{k}} S[u^2+v^2]\, du\, dv. \tag{18}$$

Adding (17) and (18), we obtain the expected edge response:

$$E\{\mathbf{O}[Q](x, y)\} = R(x) = V[1-\exp(-L-D)] + \left[\sum_{k=1}^{\infty} (1/k!) \right.$$

$$\times [L^k \exp(-L) - (L+D)^k \exp(-L-D)]$$

$$\left. \times \int_{-\infty}^{\infty} \int_{-\infty}^{-x\sqrt{k}} S[u^2+v^2]\, du\, dv \right]. \tag{19}$$

Setting $x = \pm\infty$ in (19) yields

$$R(-\infty) = V[1-\exp(-L)] \approx V \qquad \text{for large} \quad L$$

and

$$R(\infty) = V[1-\exp(-L-D)] \approx V.$$

Setting $x = 0$ we have

$$R(0) = (V/2)[2-\exp(-L)-\exp(-L-D)] \approx V.$$

So for L values in the range assumed by the theorem the edge response equals the volume constant V at $x = \pm\infty$ and at $x = 0$. Now we need to show that $R(x)$ dips below V for $x > C$ (i.e., a wrong-way Mach band begins at that point) and rises above V for $x < -C$. We show the former explicitly and then appeal to symmetry to prove the latter. Let $V(x, k)$ denote the integral in (19), i.e.,

$$V(x, k) = \int_{-\infty}^{\infty} \int_{-\infty}^{-x\sqrt{k}} S[u^2+v^2]\, du\, dv,$$

and let

$$s(x, j) = \int_{-\infty}^{\infty} \int_{-x\sqrt{j+1}}^{-x\sqrt{j}} S[u^2+v^2]\, du\, dv$$

so that

$$V(x, k) = \sum_{j=k}^{\infty} s(x, j).$$

We note that for $x > C$, $s(x, j)$ is negative for all $j \geqslant 1$, since in that case $S[u^2 + v^2]$ is negative throughout the vertical strip $-x\sqrt{j+1} \leqslant u \leqslant -x\sqrt{j}$. Now let

$$d(k) = (1/k!)[L^k \exp(-L) - (L+D)^k \exp(-L-D)];$$

i.e., $d(k)$ is the difference between $P(Q=k)$ when Q is Poisson with mean L and $P(Q=k)$ when Q is Poisson with mean $L+D$. Then Eq. (19) can be rewritten as

$$\begin{aligned} R(x) &= V[1 - \exp(-L-D)] + \sum_{k=1}^{\infty} d(k)\, V(x, k) \\ &= V[1 - \exp(-L-D)] + \sum_{k=1}^{\infty} \left[d(k) \sum_{j=k}^{\infty} s(x, k) \right] \\ &\approx V + \sum_{k=1}^{\infty} \left[d(k) \sum_{j=k}^{\infty} s(x, k) \right] \qquad \text{(for large } L\text{)} \\ &= V + \sum_{k=1}^{\infty} \left[s(x, k) \sum_{j=1}^{k} d(j) \right]. \end{aligned} \tag{20}$$

Now when L is large enough to justify replacing the cumulative Poisson distribution function with the cumulative normal distribution function N, (19) becomes

$$R(x) = V + \sum_{k=1}^{\infty} s(x, k)[N[(k-L)/\sqrt{L}] - N[(k-L-D)/\sqrt{L+D}]] \tag{21}$$

For $k > 0$ the difference between the two normal CDFs in (21) is always positive and $s(x, k)$ is always negative for $x > C$. Hence the entire sum is negative, so $R(x) < V$ for $x > C$, as claimed.

To show that a wrong-way Mach band will appear on the low side of the edge (i.e., that $R(x)$ will be $> V$ for $x < -C$) we replace L in (21) with $L' = L + D$, and D with $D' = -D$. Equation (21) still describes the edge response for large L, but now it is the response to a downwards illuminance step from $L+D$ to L at $x' = 0$. The integrals $s(x, k)$ are still all negative for $x > C$, since they do not depend on the input image, but now the difference between the normal CDFs in (21) is always negative. So each term in the sum is positive, and consequently $R(x) > V$. But the response for $x > C$ to an illuminance drop from $L+D$ to L must be the mirror image of the response for $x < -C$ to an illuminance increase from L to $L+D$, so the latter must be $> V$ for $x < -C$. ∎

5. Discussion

Mach himself (1865) attributed Mach bands to a "reciprocal action of neighboring areas of the retina" which acts like double differentiation, so that light falling on a given point exerts an excitatory effect at that point and an inhibitory effect at neighboring points. (Ratliff, 1965, reproduces Mach's papers.) He believed that the function of this process is to emphasize the borders of objects. Both ideas have generally been accepted by subsequent investigators. Constant volume operators provide an alternative mechanism for Mach bands based an entirely different motivation. From their perspective, Mach bands and other high-pass filter effects can be interpreted as by-products of a retinal process whose real function is to maximize spatial resolution in the face of photon noise. This mechanism involves only positive spatial summation—lateral excitation. And as we have seen in this paper, if one tries to combine this mechanism with lateral inhibition the resulting edge response looks quite unlike the Mach bands perceived at edges. So if one begins with the problem of photon noise and asks how the retina might be designed to maximize spatial resolution across different light levels, while maintaining a constant reliability for contrast detection, one is led to a class of operators which solve that problem and duplicate the main features of spatial vision when the pointspread function is positive, but fail rather dramatically when the pointspread contains negative lobes. In other words, if one begins with the problem of photon noise one can be led among a theoretical path in which the concept of lateral inhibition holds no attraction at all.

Writing in 1865, of course, Mach was unaware of the statistical problems confronting the visual system and had no reason to explore retinal mechanisms motivated by those problems. But the visual system itself has always had a broader perspective: its design has been shaped by photon noise from the very beginning. Is it possible that the design of the retina is based on a constant volume principle? The history of retinal physiology has been so strongly influenced by the concept of lateral inhibition that it is difficult to say how the weight of evidence would appear today if the idea of CV operators had been around from the start. Current physiological accounts are based firmly on lateral inhibition, and the notion of a CV operation simply does not arise. However, if one examines the physiological data with an open mind, it is surprisingly difficult to find evidence that unequivocally rules out a CV interpretation. At a qualitative level the responses of retinal ganglion cells driven by a CV mechanism would look like those observed in electrophysiology: at moderate to high light levels ganglion cells would appear to have a receptive field divided into antagonistic center and surround regions, and at very low levels the receptive field would appear to consist only of a positive central zone, with no inhibitory surround. So a CV interpretation cannot be immediately rejected on the basis of physiology.

A detailed comparison between psychophysical data and CV predictions for Poisson-noisy input images shows that while the Gaussian CV model duplicates the main qualitative properties of spatial vision, it fails to match human performance

quantitatively in certain critical respects (Yellott, 1987). In particular, it incorrectly implies that as retinal illuminance rises in the photopic range, the CSF should simply shift bodily to the right along the log spatial frequency axis, as shown here in Fig. 10. It this were true, contrast sensitivity would decrease at low spatial frequencies as mean retinal illuminance rises. That would be an undesirable side-effect, and it does not occur empirically (Van Nes and Boumann, 1967). However the CV model analyzed in that paper (the same model considered here in Section 4) is far too stark to be realistic. For example, it does not involve any temporal component: it treats retinal image processing on a frame-by-frame basis and ignores the fact that in a real retina the pointspread function would develop over time. Cornsweet and Reumann (1986) have studied the consequences of adding a time component to CV operators. They find that the resulting model can duplicate many of the well known temporal properties of human vision. At present it is not obvious whether the psychophysical defects of CV operators as visual models can be cured by tinkering with temporal assumptions: more work needs to be done on this problem.

For the moment then, one can argue that it is an open question whether a CV-like mechanism has any physiological reality. But even if it turns out that evolution has made no use of CV operators and designed the retina along completely different lines, these operators would still be of interest to visual science because they are motivated by fundamental design considerations, i.e., by problems faced by all visual systems, whether biological or manmade. And they provide a simple solution to those problems—a solution that could readily be implemented by hardware and should prove useful in machine vision. For that reason alone it seems worthwhile to develop their theory. As we noted at the outset (and as is apparent throughout this paper), that theory is still in rough form: the main consequences of image processing by CV operators have been worked out by a mixture of homespun mathematics and computation, but much remains to be done to create a polished general theory. The results of this paper show at least that one direction which might have seemed intuitively promising needs no further exploration: we know that nothing useful can be achieved by combining CV operators and lateral inhibition.

REFERENCES

AGUILAR, M., & STILES, W. S. (1954). Saturation of the rod mechanism of the retina at high levels of stimulation. *Optica Acta*, **1**, 59–64.

BARLOW, H. B. (1957). Increment thresholds at low intensities considered as signal/noise discriminations. *Journal of Physiology*, **136**, 469–488.

BARLOW, H. B. (1958). Temporal and spatial summation in human vision at different background intensities. *Journal of Physiology*, **141**, 337–350.

BAYLOR, D. A., NUNN, B. J., & SCHNAPF, J. L. (1984). The photocurrent, noise, and spectral sensitivity of rods of the monkey macaca fasicularis. *Journal of Physiology*, **357**, 575–607.

BOSMAN, D., BOTERENBROOD, H., & VAN HUIJSTEE (1985). Two non-linear image enhancement algorithms. *Department of Electrical Engineering*, Twente University of Technology.

CORNSWEET, T. N., & REUMAN, S. (1986). CVIDS—A new model for spatio-temporal interactions. *Investigative Opthalmology and Visual Science*, 27, **3**, 226. [Abstract]

CORNSWEET, T. N., & YELLOTT, J. I., JR. (1985). Intensity-dependent spatial summation. *Journal of the Optical Society of Amerika-A*, **2**, 1769–1786. [Errata: *J. Opt. Soc. Am.-A*, 1986, p. 165.]

DEVRIES, H. (1943). The quantum character of light and its bearing upon threshold of vision, the differential sensitivity and visual acuity of the eye. *Physica*, **11**, 179–189.

ENROTH-CUGELL, C., & ROBSON, J. G. (1966). The contrast sensitivity of the ganglion cells of the cat. *Journal of Physiology*, **187**, 517–552.

GLEZER, V. D. (1965). The receptive fields of the retina. *Vision Research*, **5**, 497–525.

HESS, R. F., & NORDBY, K. (1986). Spatial and temporal limits of vision in the achromat. *Journal of Physiology*, **371**, 365–385.

MACH, E. (1865). Über die wirkung der räumlichen vertheilung des lichtreizes auf die netzhaut. *Sitzungsberichte der mathematischnaturwissenschaftlichen Class der kaiserlichen Akademic der Wissenschaften*, Wein, 52/2, 303–322; reproduced in English in RATLIFF, F. (1965). *Mach bands: quantitative studies on neural networks in the retina.* San Francisco: Holden–Day.

MARR, D., & HILDRETH, E. (1980). Theory of edge detection. *Proceedings of the Royal Society of London*, **207**, 187–217.

PIRENNE, M. H. (1967). *Vision and the eye.* London: Chapman & Hall.

RATLIFF, F. (1965). *Mach bands: Quantitative studies on neural networks in the retina.* San Francisco: Holden–Day.

ROSE, A. (1942). The relative sensitivities of television pickup tubes, photographic film and the human eye. *Proceeding of the I.R.E.*, **30**, 293–300.

ROSE, A. (1948). The sensitivity performance of the human eye on an absolute scale. *Journal of the Optical Society of America*, **38**, 196–208.

SHADE, O. H. (1956). Optical and photoelectric analog of the eye. *Journal of the Optical Society of America*, **46**, 721–739.

THOMAS, J. P. (1975). Spatial resolution and spatial interaction. In E. C. Cartertette and M. P. Friedman (Eds.), *Handbook of Perception* (Vol. 5). New York: Academic Press.

VAN NES, F. L., & M. A. BOUMAN, M. A. (1967). Spatial modulation transfer in the human eye. *Journal of the Optical Society of America*, **12**, 89–101.

YELLOTT, J. I., JR. (1987). Photon noise and constant volume operators. *Journal of the Optical Society of America-A*, **4**, 2418–2446.

RECEIVED: April 25, 1986